DOI: 10.1002/anie.200902073

Microscopy

Super-Resolution Imaging with Small Organic Fluorophores**

Mike Heilemann, Sebastian van de Linde, Anindita Mukherjee, and Markus Sauer**

Fluorescence imaging has become an essential tool in biological and biomedical sciences for three-dimensional (3D) imaging of living cells and tissues. In contrast to other imaging techniques such as electron microscopy, fluorescence microscopy offers an advantage because it enables imaging even of dynamic processes in living cells. The weakness, however, has been the fact that the spatial resolution was limited to approximately 200 nm in the imaging plane.[1] Only recently have methods emerged that enable subdiffraction-resolution imaging based on photoswitchable or photoactivatable fluorescent proteins and organic fluorophores.[2] Currently, most super-resolution approaches control fluorescence emission of fluorophores by modulating their transition between a fluorescent (on) and nonfluorescent (off) state.[2–10]

However, super-resolution imaging with commercially available small organic fluorophores remains challenging. Herein we introduce a novel and facile method that enables super-resolution imaging with standard Alexa Fluor and ATTO dyes. We demonstrate that these frequently used fluorophores, which span the visible wavelength range, can be switched reversibly between an on and an off state under similar experimental conditions. The protocol we developed comprises solely the addition of thiol-containing reducing agents such as β-mercaptoethylamine (MEA), dithiothreitol (DTT), or glutathione (GSH), which efficiently populate a relatively stable nonfluorescent state. Since oxygen does not have to be removed and reducing agents such as glutathione are present in the cytoplasm of cells in the micromolar to millimolar range, the method we describe is very relevant for super-resolution imaging with molecular-scale resolution (ca. 20 nm) even in living cells.

Single-molecule-based localization methods combine photoactivation or reversible photoswitching and precise position determination of individual fluorescent spots to reconstruct a super-resolution image.[5–15] Photoswitchable fluorophores (photoswitches) are used in various single-molecule-based super-resolution imaging methods, such as photoactivated localization microscopy (PALM),[5] fluorescence photoactivation localization microscopy (FPALM),[6] stochastic optical reconstruction microscopy (STORM),[8] and direct STORM (dSTORM).[10] The experimental procedure of all these methods is similar: a sample is densely labeled with a photoswitchable fluorophore, for example by immunocytochemistry or coexpression of a fluorescent protein, and prepared such that most fluorophores are in their off state and only a subset of fluorophores is fluorescent at a given time. The emission profiles of single emitters are localized through the approximation with a Gaussian fit with a precision that is determined by the number of photons detected and the background fluorescence, that is, autofluorescence of the sample and residual fluorescence of surrounding fluorophores in the off state.[16] Thus, photoswitches with a high intensity contrast between the on and off states, together with high extinction coefficients and quantum yields in the on state, are the key for nanometer accuracy. The repetitive cycling of photoactivation, localization, and deactivation of individual fluorophores allows the reconstruction of fluorescence images with an experimental resolution of 20 nm or slightly better.[8–10,12–14]

Since small organic fluorophores such as rhodamine derivatives exhibit higher fluorescence count rates in the on state than fluorescent proteins (FPs), they appear to be the fluorophores of choice for super-resolution imaging. Moreover, a huge selection of organic fluorophores with different spectral characteristics and chemical modifications is commercially available. Conjugation to small receptor-binding peptides, short DNA or RNA fragments or hairpins, whole proteins, and even small drug molecules is possible with standard chemistry. In combination with new tag technologies[17,18] small organic fluorophores can even be specifically attached to target proteins in living cells to perform live-cell imaging. Therefore, new methods combining genetic labeling and organic fluorophores are well-suited for super-resolution fluorescence imaging.

In general, super-resolution imaging with small organic fluorophores requires that the majority of fluorophores can be transferred into a stable off state with practically zero quantum yield, that is, conditions must be established that enable the temporally isolated readout and localization of a subset of individual fluorophores residing in the on state. This prerequisite can be achieved by using a light-induced process to generate off states that exhibit a survival time (lifetime) which is substantially longer than the lifetime of the bright on state. Rhodamine amide derivatives that can be photoactivated upon excitation with UV radiation[11] as well as long-lived triplet states in rhodamine derivatives have been used successfully for super-resolution imaging.[9] However, to prolong the lifetime of the triplet state, the samples must be embedded in a poly(vinyl alcohol) matrix with low oxygen permeability. Furthermore, relatively high excitation intensities (greater than 10 kW cm^{-2}) must be applied. Likewise, it

[*] Dr. M. Heilemann, S. van de Linde, Dr. A. Mukherjee, Prof. Dr. M. Sauer
Applied Laser Physics & Laser Spectroscopy, Bielefeld University
Universitätsstrasse 25, 33615 Bielefeld (Germany)
Fax: (+49) 521-106-2958
E-mail: heileman@physik.uni-bielefeld.de
sauer@physik.uni-bielefeld.de
Homepage: http://www.physik.uni-bielefeld.de/experi/d3/

[**] This work was supported by the Biophotonics and the Systems Biology Initiative (FORSYS) of the German Ministry of Research and Education (BMBF, grants 13N9234 and 0315262).

Supporting information for this article is available on the WWW under http://dx.doi.org/10.1002/anie.200902073.

has been demonstrated that the generation of radical anions in carbocyanine derivatives can be used for super-resolution imaging.[14] Nevertheless, the generation of long-lived off states in organic fluorophores remains challenging and to date requires the removal of oxygen and the addition of fluorophore-specific oxidizing and reducing agents, which prevents its use for live-cell applications.[8,10,14,19,20]

On the other hand, it has been shown that some red-absorbing fluorophores can be switched reversibly between a fluorescent and a nonfluorescent state in the presence of oxygen and β-mercaptoethylamine.[12] On the basis of these findings and the knowledge that the fluorescence emission of most rhodamine and oxazine derivatives is efficiently quenched by collision with electron donors such as the amino acid tryptophan and the nucleobase guanosine,[21–26] we intended to develop a universal, widely applicable method for super-resolution imaging with small organic fluorophores under physiological conditions.

With the exception of some carbocyanine dyes such as Cy3, Cy5, and Alexa Fluor 647, most commercial fluorophores with absorption maxima between 480 and 700 nm belong to the class of rhodamine and oxazine derivatives. Because they feature the same basic chromophore structure,[27] they exhibit similar redox properties.[21,23,28] In other words, it should be possible to find experimental conditions under which fluorescence quenching of rhodamine and oxazine fluorophores can be used advantageously for reversible photoswitching.

Inspired by these ideas, we performed fluorescence quenching experiments with various Alexa Fluor and ATTO dyes and different electron donors, with the intention of finding reducing agents that selectively quench the energetically slightly stabilized triplet state but leave the singlet state unaffected. We found that reducing agents with thiol groups, such as MEA, DTT, and GSH, selectively quench the triplet state of rhodamine and oxazine derivatives depending on the pH value of the aqueous buffer used. Since most thiols (RSH) have a $pK_{a(SH)}$ 8–9[29–31] and the reducing species is the thiolate anion (RS^-), the reduction efficiency of compounds carrying one thiol group exhibits a plateau at pH > 9, above which the thiol group is ionized, and a corresponding linear increase in reduction potential with a decrease in pH value. The first excited singlet state of ATTO655 is quenched by electron transfer from various thiol compounds (RSH/RS^-) only at pH > 9 (Figure 1a). The triplet state, however, is energetically stabilized and thus quenched by RSH/RS^- even at pH 7–8. Furthermore, the thiolate (RS^-) competes with oxygen, which is known to efficiently quench triplet states[20] and is present at approximately 250 μM concentration under standard conditions in aqueous solution.[32] As a consequence, the pH value of the solvent and the thiol concentration are crucial experimental parameters, and efficient quenching of the triplet state under physiological conditions (pH 7–8) requires a concentration of 10–100 mM thiol (Figure S1a in the Supporting Information).

The radical anions formed in the first reaction step can be reoxidized by molecular oxygen or can further react to other very stable nonfluorescent species that exhibit a lifetime of several hundred milliseconds even in the presence of oxygen

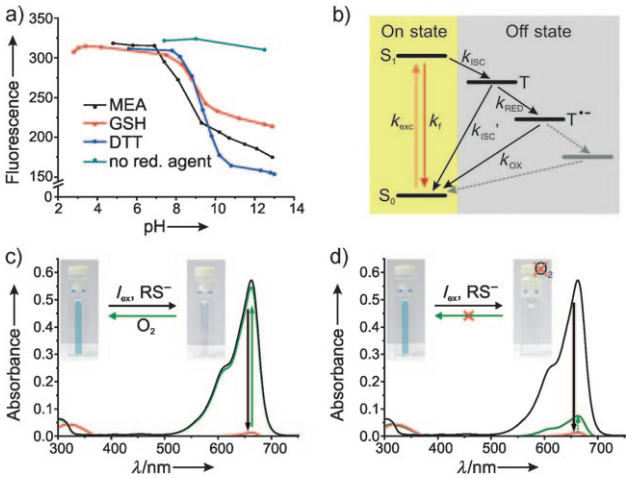

Figure 1. Principle of photoswitching with small organic fluorophores exemplified by ATTO655. a) Fluorescence quenching of ATTO655 in 100 mM MEA, GSH, and DTT with increasing pH value (addition of KOH). The green curve was obtained in the absence of thiol in phosphine-buffered saline (PBS; pH 7.4) or 100 mM potassium borate buffer (pH 9.0 and 12.5) and demonstrates a slight decrease in fluorescence intensity of ATTO655 owing to nucleophilic addition by solvent molecules at higher pH values. b) Underlying photophysical processes of reversible photoswitching of Alexa Fluor and ATTO dyes. After excitation of the fluorophores (k_{exc}) into their first excited singlet state S_1, the excited-state energy is either released through fluorescence emission with rate k_f, or the triplet state is occupied (k_{ISC}). The triplet state T is either depopulated (k_{ISC}') or reduced by thiolate RS^- (k_{RED}) to form radical anion $T^{\bullet-}$, which is reoxidized by molecular oxygen with rate k_{OX} or reacts to other nonfluorescent species. c,d) Absorption spectra of ATTO655 in the presence of 100 mM MEA at pH 9.3 under irradiation of ATTO655 at 658 nm with an excitation intensity of 140 mW cm^{-2} (see text for details).

(Figure 1b and Figure S3a,b in the Supporting Information). The irradiation of an aqueous solution of ATTO655 with 100 mM MEA at pH 9.3 completely transfers the fluorophores into stable nonfluorescent species (red curve in Figure 1c) within a few minutes. The original colored form, however, can be easily recovered almost completely by gently agitating the solution (green curve in Figure 1c). This finding implies two results: 1) Oxygen or other oxidizing agents (Figure S1b in the Supporting Information) are responsible for generating the on state and are consumed with proceeding reaction. 2) The off state is thermally very stable. These conclusions are further corroborated by the fact that the colored form cannot be recovered efficiently when oxygen is removed from the solution by purging with nitrogen prior to irradiation (Figure 1d).

According to these results, the reaction of RS^- with the triplet states of fluorophores produces radical anions and thiyl radicals ($T + RS^- \rightarrow T^{\bullet-} + RS^{\bullet}$). The main reactions of thiyl radicals in aqueous solution are conjugation with thiols or thiolates, dimerization to the corresponding disulfides, or reaction with molecular oxygen.[30,33] The free-radical reactions can generate superoxide radicals and hydrogen peroxide. Depending on the experimental conditions, other very stable nonfluorescent species can be formed in follow-up

reactions. Both radical anions and other reduced species are transferred efficiently to the fluorescent state upon reaction with oxygen. As the formation of superoxide radicals and hydrogen peroxide is less efficient, the main consequence of the reaction mechanism is oxygen consumption. Both thiol oxidation and oxygen consumption have been shown to increase with pH value as a consequence of the increasing fraction of thiolate in the reaction medium.[30,33]

Reversible photoswitching at the ensemble level allows us to study the reaction mechanism in more detail in simple fluorescence experiments. The fluorophores can be reversibly switched between an on and an off state many times and with minimal loss in fluorescence intensity after recovery (Figure 2a). In these experiments, ATTO655 was dissolved at a concentration of 10^{-6} M in water containing 100 mM MEA and irradiated at 658 nm with an excitation intensity of 110 mW (ca. 140 mW cm^{-2}). Formation of the off state results in an almost exponential decrease in fluorescence intensity, of which large parts can be approximated by an exponential model (red curve, Figure 2b) to extract an off rate constant k_{off}. It should be pointed out that the decay curve is superimposed by diffusion processes, and off-state formation is accompanied by oxygen and hydrogen peroxide production.

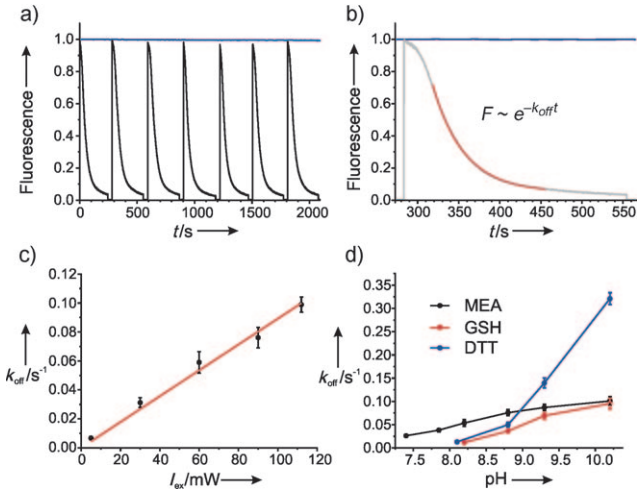

Figure 2. Photoswitching of ATTO655. a) Irradiation of ATTO655 at 658 nm with an excitation intensity of 140 mW cm^{-2} in the presence (black) and absence (blue) of 100 mM MEA (pH 7.4). The fluorescence was recovered by gently agitating the solution. b) A large portion of the decrease in fluorescence intensity can be approximated by a monoexponential function to extract the off rate k_{off}. c) The off rate k_{off} of ATTO655 shows a linear dependence on excitation intensity in the range of 6–140 mW cm^{-2} (100 mM MEA at pH 9.3). d) Dependence of the off rate on pH value for MEA, GSH, and DTT (140 mW cm^{-2}, 658 nm).

Although inefficient, these side reactions contribute to the observed fluorescence decay and complicate fitting procedures, for which reason we limited fitting to the central part of the decay curve. In the absence of thiol the fluorescence intensity remains constant (blue curve in Figure 2a,b). Upon opening of the cuvette, fresh oxygen is dissolved and the fluorescent state is efficiently recovered within seconds upon agitation. Photoswitching between the on and off states is highly reversible (Figure 2a). The fluorescent state of more than 95% of all fluorophores can be recovered even after 10 switching cycles. This result demonstrates that aggressive species such as superoxide radicals and hydrogen peroxide are produced at very low concentrations even in ensemble experiments.

As expected for a light-induced process, the formation of fluorophore radical anions and secondary products is mainly determined by the irradiation intensity in the presence of adequate concentrations of RS^-. Consequently, the off rate increases linearly with increasing excitation intensity in the range of 6–140 mW cm^{-2} in the presence of 100 mM MEA at pH 9.3 (Figure 2c). Furthermore, k_{off} measured for ATTO655 in the presence of 100 mM MEA, DTT, and GSH increases dramatically with increasing pH value (Figure 2d). Measurements at pH > 10.2 were not interpreted, as some fluorophores (e.g., ATTO655) are irreversibly destroyed, most probably owing to a nucleophilic addition of OH^- at higher pH values (see also fluorescence intensity of ATTO655 in the absence of RS^- at pH > 10 in Figure 1a). Owing to the faster formation of radical anions at higher pH values, ensemble experiments shown in Figure 1c,d were performed at pH 9.3. While the monothiols MEA and GSH show an almost linear dependence of k_{off} with pH value, dithiol DTT shows a more pronounced pH dependence (Figure 2d). Thus, the pH value of the solution offers an elegant parameter to adjust the lifetime of the on state. On the other hand, the lifetime of the off state is controlled by the redox properties of the fluorophores as well as by the oxygen concentration and the oxygen accessibility of the fluorophore.

Building on the result that millimolar concentrations of thiol compounds in aqueous solutions allow reversible, facile switching of small organic fluorophores, we performed super-resolution imaging of the cytoskeletal network of fixed cells with an exemplary selection of eight different organic fluorophores (Figure 3). For immunofluorescence imaging of microtubules, COS-7 cells were stained with primary antibodies and then with fluorescently labeled secondary antibodies. Whereas antibodies labeled with Alexa Fluor 488, Alexa Fluor 532, and Alexa Fluor 568 are commercially available with between three and six fluorophores per antibody, Fab fragments labeled with ATTO520, ATTO565, ATTO590, ATTO655, and ATTO700 were assembled with a labeling degree of one or two according to standard procedures. Fluorescence images were recorded by total internal reflection fluorescence (TIRF) microscopy. Depending on their absorption maxima, fluorophores were excited at 488 nm (Alexa Fluor 488), 514 nm (ATTO520 and Alexa Fluor 532), 568 nm (ATTO565, ATTO590, and Alexa Fluor 568), or 647 nm (ATTO655 and ATTO700). The same antibodies can be used successfully as secondary antibodies to label other cellular structures (Figure S2 in the Supporting Information).

The laser intensities were adjusted to ensure that the lifetime of the off state is substantially longer than the lifetime of the on state (Figure S3a,b in the Supporting Information). Thus, only a subset of fluorophores is activated at any given

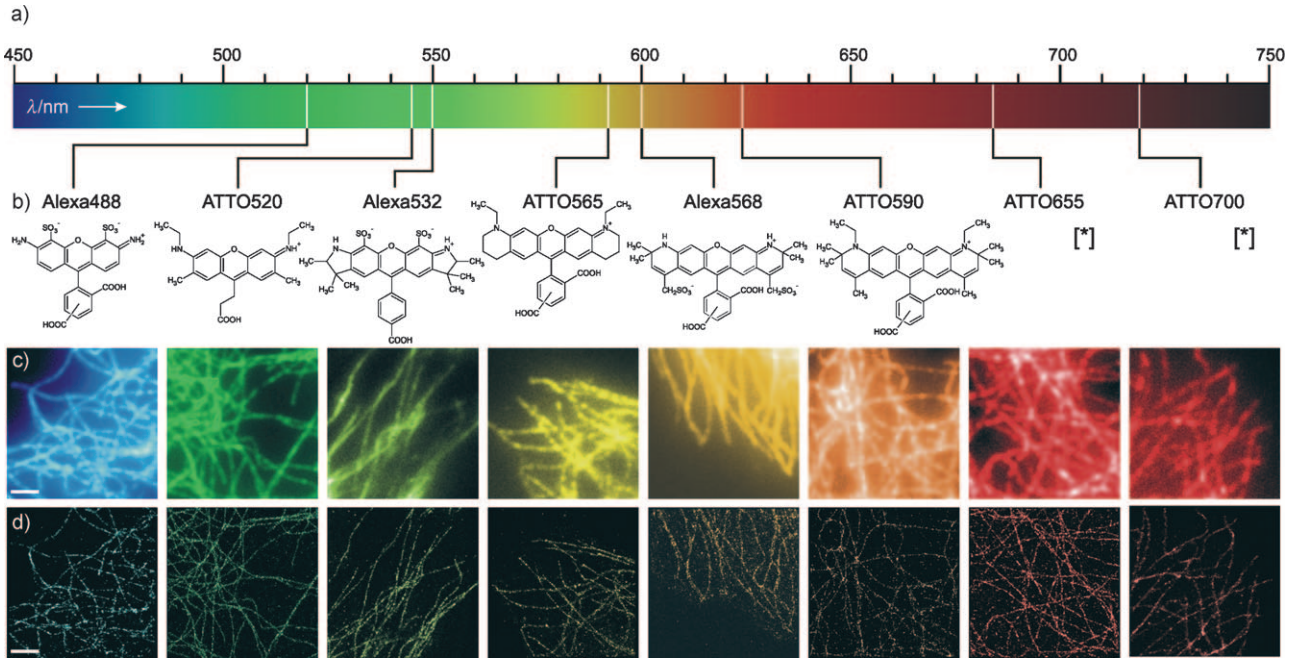

Figure 3. Super-resolution imaging of the cytoskeletal network of mammalian cells with eight different Alexa Fluor and ATTO dyes spanning the visible wavelength range according to the dSTORM principle.[10] a, b) Emission maxima and molecular structures of the eight fluorophores Alexa Fluor 488, ATTO520, Alexa Fluor 532, ATTO565, Alexa Fluor 568, ATTO590, ATTO655, and ATTO700 ([*] molecular structures are not available). c) Immunofluorescence images (TIRF microscopy) of microtubules in COS-7 cells (scale bar 2 μm) and d) corresponding reconstructed super-resolution images. Experiments were performed in PBS, pH 7.4, 10–200 mM MEA, with a frame rate of 10–20 Hz and excitation intensities of 1–4 kW cm^{-2} (matched to balance the different extinction coefficients of the fluorophores at the excitation wavelength). Alexa Fluor 488: 488 nm, 3 kW cm^{-2}, 100 mM MEA; ATTO520: 514 nm, 3 kW cm^{-2}, 100 mM MEA; Alexa Fluor 532: 514 nm, 1.5 kW cm^{-2}, 100 mM MEA; ATTO565: 568 nm, 1.5 kW cm^{-2}, 100 mM MEA; Alexa Fluor 568: 568 nm, 1.5 kW cm^{-2}, 100 mM MEA; ATTO590: 568 nm, 4 kW cm^{-2}, 200 mM MEA; ATTO655: 647 nm, 1.5 kW cm^{-2}, 10 mM MEA; ATTO700: 647 nm, 4 kW cm^{-2}, 100 mM MEA.

time in the field of view. The resulting point-spread function measured from each fluorophore residing in the on state was analyzed by fitting a Gaussian function to localize its position with high precision. After thousands of position determinations (localizations), the super-resolution image was reconstructed. The super-resolution images (Figure 3d) show substantially better spatial resolution than the images in Figure 3c for all fluorophores. Typically, we recorded 10000–20000 frames at frame rates of 10–33 Hz and achieved an optical resolution of approximately 20 nm (Figure S3c in the Supporting Information). Higher frame rates can be achieved using faster EMCCD cameras in combination with higher excitation intensities. Under the applied experimental conditions, all tested fluorophores exhibit fluorescence count rates of 10–30 kHz. Thus, 500–3000 photons can be used to calculate fluorophore localizations with a theoretical precision of 5–15 nm.[16]

At this point, we must consider that the achievable resolution is not only controlled by the number of photons and the mechanical stability of the setup but also by the labeling density. According to the Nyquist–Shannon sampling theorem,[34] the mean distance between neighboring localized molecules must be at least half of the desired resolution. To achieve an optical resolution of 20 nm, a mean distance between neighboring fluorescently labeled antibodies of 10 nm or less is required, which is rather challenging considering that the size of a typical IgG antibody is about 7 nm. The theoretical maximum resolution is further deteriorated as most immunofluorescence assays use both a primary and a secondary antibody. In this respect, the use of photoactivatable or photoswitchable fluorescent proteins (FPs) is advantageous, because they enable higher labeling densities owing to their comparably small size. On the other hand, FPs often exhibit lower photostability than conventional organic fluorophores. Furthermore, even though they are smaller than antibodies, the size of the FP tag (e.g., 27 kDa for GFP) may in some cases still affect the function of the target protein. The advantage of small organic fluorophores for super-resolution imaging lies in the variability of their use.

As can be seen in Figure 2d, super-resolution imaging with small organic fluorophores is not restricted to the use of MEA but also works with other thiols such as GSH under physiological conditions. The tripeptide GSH is the most abundant low-molecular-weight thiol protectant and antioxidant in mammalian biology. The thiol groups are kept in a reduced state at millimolar concentrations in animal cells.[35] Encouraged by these considerations, we performed live-cell super-resolution imaging experiments with small organic fluorophores such as ATTO655, ATTO680, ATTO700, and ATTO520 (Figure 4 and Figure S4 in the Supporting Information) that exhibit the most pronounced electron-accepting properties and therefore require only low millimolar concentrations of thiols to be efficiently transferred to the long-lived off state.

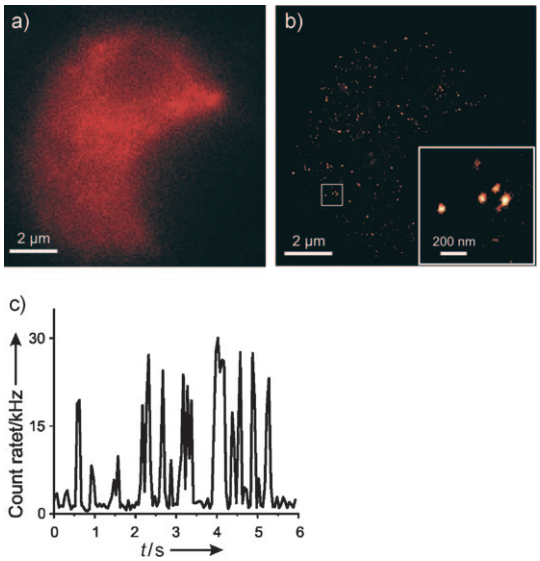

Figure 4. Super-resolution imaging of mRNA in living A549 cells with oligo(dT) 43-mers labeled with ATTO655. a) Conventional fluorescence image (TIRF microscopy) of the nucleus of a living A549 cell showing that oligonucleotides enter the cell and generate a homogeneous fluorescence signal. b) Reconstructed super-resolution fluorescence image measured by excitation at 647 nm with an intensity of 1.5 $kW cm^{-2}$ at a frame rate of 20 Hz. c) Fluorescence time trace of a fluorescent spot as shown in the expanded super-resolution image in (b) most likely comprising more than one fluorophore. The time trace demonstrates that ATTO655 and other small organic fluorophores (Supporting Information, Figure 3S) can be used as reversible photoswitches in living cells.

Although a lot of effort is still being put into optimizing RNA in situ hybridization procedures on fixed cells and tissue materials, there is an increasing demand for techniques that allow the visualization of RNA in living cells to determine whether the observed RNA localization patterns in fixed cells reflect the situation in living cells. Fixation and cell pretreatment may disturb localization patterns and to some extent deteriorate cell morphology.[36,37]

To target RNA in living cells, the target sequence has to be labeled with a complementary sequence that carries a fluorescent probe. In our experiments, A549 cells were transfected with fluorescently labeled oligo(dT) 43-mers and imaged after washing with cell culture medium (Figure 4). As oligo(dT) is expected to bind to poly(A) RNA sequences, RNA monitoring of labeled 43-mer oligo(dT) is a direct measure of mRNA mobility and localization in the nucleus. At very low excitation intensity (ca. 0.1 $kW cm^{-2}$) the fluorescence signal is homogeneously smeared over the nucleus (Figure 4a) and reports that the cell is successfully transfected with fluorescently labeled oligonucleotides. By increasing the excitation intensity to 1.5 $kW cm^{-2}$ most fluorophores are switched off by reduction of the triplet sate by GSH. Fluorophores are reversibly switched between the on and off states (Figure 4c), thus enabling super-resolution imaging of mRNA in living cells with standard small organic fluorophores. The super-resolution image shows distinct fluorescence signals and clusters localized in the nucleus that appear as immobile spots on the time scale of the experiment (ca. 500 s, Figure 4b). The molecules are immobile in the nucleoplasm, most probably owing to binding to nuclear proteins or other obstacles.[38,39] Furthermore, some reports demonstrated that oligo(dT) can interact at least transiently with nuclear speckle domains[36,37] or immobile elements of the transcriptional, splicing, or polyadenylation machinery.[40]

Our results demonstrate super-resolution imaging with commercially available small organic fluorophores in cells using a universally valid protocol. Consequently, the list of organic fluorophores that can be used for super-resolution imaging can be extended to all common rhodamine and oxazine derivatives from the blue to the red part of the electromagnetic spectrum. The underlying mechanism can be described as remarkably efficient cycling between a fluorescent and nonfluorescent state of the fluorophores in the presence of millimolar concentrations of thiols. As demonstrated, the lifetime of the on state can be adjusted by the excitation intensity, provided that the concentration of the reducing thiolate species ensures efficient quenching of the triplet state by formation of radical anions and subsequent secondary reactions to a stable off state.

The lifetime of the off state, that is, the time it takes until the reduced species are oxidized by oxygen to repopulate the singlet state, is predetermined by the oxygen concentration. Nevertheless, the average lifetime of the off state can be reduced by using antibodies that carry more fluorophores, that is, by increasing the degree of labeling. In that case, the lifetime of the off state of an "antibody" is stochastically determined by the number of fluorophores attached. In combination with higher excitation intensities, the lifetime of the on and off states can be reduced to enable higher imaging speeds. However, higher excitation intensities will promote light-induced cell damage.

Although the pH value and GSH concentration of cells will vary strongly between different cell types and conditions, the method presented herein is suitable for live-cell experiments using selected fluorophores such as ATTO520, ATTO655, ATTO680, and ATTO700 (Figure 4 and Figures 3S and 4S in the Supporting Information). Importantly, the method enables screening for suited live-cell fluorophores by simple ensemble cuvette experiments. The intriguing simplicity of the method facilitates its application and opens avenues for multicolor super-resolution imaging with combinations of small organic fluorophores. Our results indicate that the development of new methods combining the genetic labeling approach with small, bright, and photostable organic fluorophores represents the method of choice for future super-resolution imaging and precision colocalization experiments.

Received: April 17, 2009
Revised: May 29, 2009
Published online: August 7, 2009

Keywords: diffraction limit · dyes/pigments · live-cell imaging · photoswitching · super-resolution imaging

[1] E. Abbe, *Arch. Mikrosk. Anat.* **1873**, *9*, 413.
[2] S. W. Hell, *Science* **2007**, *316*, 1153.
[3] S. W. Hell, J. Wichmann, *Opt. Lett.* **1994**, *19*, 780.
[4] S. W. Hell, M. Kroug, *Appl. Phys. B* **1995**, *60*, 495.
[5] E. Betzig, G. H. Patterson, R. Sougrat, O. W. Lindwasser, S. Olenych, J. S. Bonifacino, M. W. Davidson, J. Lippincott-Schwartz, H. F. Hess, *Science* **2006**, *313*, 1642.
[6] S. T. Hess, T. P. Girirajan, M. D. Mason, *Biophys. J.* **2006**, *91*, 4258.
[7] P. Dedecker, J. Hotta, C. Flors, M. Sliwa, H. Uji-i, M. B. Roeffaers, R. Ando, H. Mizuno, A. Miyawaki, J. Hofkens, *J. Am. Chem. Soc.* **2007**, *129*, 16132.
[8] M. Bates, B. Huang, G. T. Dempsey, X. Zhuang, *Science* **2007**, *317*, 1749.
[9] J. Fölling, M. Bossi, H. Bock, R. Medda, C. A. Wurm, B. Hein, S. Jakobs, C. Eggeling, S. W. Hell, *Nat. Methods* **2008**, *5*, 943.
[10] M. Heilemann, S. van de Linde, M. Schuttpelz, R. Kasper, B. Seefeldt, A. Mukherjee, P. Tinnefeld, M. Sauer, *Angew. Chem.* **2008**, *120*, 6266; *Angew. Chem. Int. Ed.* **2008**, *47*, 6172.
[11] M. Bossi, J. Folling, V. N. Belov, V. P. Boyarskiy, R. Medda, A. Egner, C. Eggeling, A. Schonle, S. W. Hell, *Nano Lett.* **2008**, *8*, 2463.
[12] S. van de Linde, R. Kasper, M. Heilemann, M. Sauer, *Appl. Phys. B* **2008**, *93*, 725.
[13] S. van de Linde, M. Sauer, M. Heilemann, *J. Struct. Biol.* **2008**, *164*, 250.
[14] C. Steinhauer, C. Forthmann, J. Vogelsang, P. Tinnefeld, *J. Am. Chem. Soc.* **2008**, *130*, 16840.
[15] M. Heilemann, P. Dedecker, J. Hofkens, M. Sauer, *Laser Photonics Rev.* **2009**, *3*, 180.
[16] R. E. Thompson, D. R. Larson, W. W. Webb, *Biophys. J.* **2002**, *82*, 2775.
[17] I. Chen, A. Y. Ting, *Curr. Opin. Biotechnol.* **2005**, *16*, 35.
[18] M. Fernández-Suárez, A. Y. Ting, *Nat. Rev. Mol. Cell Biol.* **2009**, *9*, 929.
[19] M. Heilemann, E. Margeat, R. Kasper, M. Sauer, P. Tinnefeld, *J. Am. Chem. Soc.* **2005**, *127*, 3801.
[20] J. Vogelsang, R. Kasper, C. Steinhauer, B. Person, M. Heilemann, M. Sauer, P. Tinnefeld, *Angew. Chem.* **2008**, *120*, 5545; *Angew. Chem. Int. Ed.* **2008**, *47*, 5465.
[21] M. Sauer, K.-T. Han, R. Müller, S. Nord, A. Schulz, S. Seeger, J. Wolfrum, J. Arden-Jacob, G. Deltau, N. J. Marx, C. Zander, K. H. Drexhage, *J. Fluoresc.* **1995**, *5*, 247.
[22] J. P. Knemeyer, N. Marme, M. Sauer, *Anal. Chem.* **2000**, *72*, 3717.
[23] N. Marmé, J. P. Knemeyer, M. Sauer, J. Wolfrum, *Bioconjugate Chem.* **2003**, *14*, 1133.
[24] H. Neuweiler, A. Schulz, M. Bohmer, J. Enderlein, M. Sauer, *J. Am. Chem. Soc.* **2003**, *125*, 5324.
[25] H. Neuweiler, M. Sauer, *Curr. Pharm. Biotechnol.* **2004**, *5*, 285.
[26] H. Neuweiler, S. Doose, M. Sauer, *Proc. Natl. Acad. Sci. USA* **2005**, *102*, 16650.
[27] V. Buschmann, K. D. Weston, M. Sauer, *Bioconjugate Chem.* **2003**, *14*, 195.
[28] T. Heinlein, J. P. Knemeyer, O. Piestert, M. Sauer, *J. Phys. Chem. B* **2003**, *107*, 7957.
[29] W. W. Cleland, *Biochemistry* **1964**, *3*, 480.
[30] U. Burner, W. Jantschko, C. Obinger, *FEBS Lett.* **1999**, *443*, 290.
[31] E. Madej, P. Wardman, *Arch. Biochem. Biophys.* **2007**, *462*, 94.
[32] R. C. Weast, Chemical Rubber Company, **1979**.
[33] U. Burner, C. Obinger, *FEBS Lett.* **1997**, *411*, 269.
[34] C. E. Shannon, *Proc. IRE* **1949**, *37*, 10.
[35] H. Sies, *Free Radical Biol. Med.* **1999**, *27*, 916.
[36] R. W. Dirks, C. Molenaar, H. J. Tanke, *Histochem. Cell Biol.* **2001**, *115*, 3.
[37] C. Molenaar, A. Abdulle, A. Gena, H. J. Tanke, R. W. Dirks, *J. Cell Biol.* **2004**, *165*, 191.
[38] J. P. Leonetti, N. Mechti, G. Degols, C. Gagnor, B. Lebleu, *Proc. Natl. Acad. Sci. USA* **1991**, *88*, 2702.
[39] J. C. Politz, E. S. Browne, D. E. Wolf, T. Pederson, *Proc. Natl. Acad. Sci. USA* **1998**, *95*, 6043.
[40] J. P. Knemeyer, D. P. Herten, M. Sauer, *Anal. Chem.* **2003**, *75*, 2147.

